Stray Capacitance Modeling of Inductors by Using the Finite Element Method

Qin Yu
Lucent Technologies, Inc.*
6200 E. Broad Street
Columbus, OH, USA

Thomas W. Holmes
Hewlett-Packard Co.*
7887 Washington Village Dr.
Dayton, OH, USA

Abstract: Stray capacitance modeling of an inductor is essential for its accurate equivalent circuit modeling. The stray capacitance determines the inductor's performance and upper frequency limit. In this paper, a method is proposed for modeling the distributed stray capacitance of inductors by the finite element method and a node-to-node lumped capacitance network. The effects of the wire insulation layer, ferrite core, the number of segments used to model the circumference of the wire cross section, the pitch and coil-to-core distances, and the capacitance between non-adjacent turns, etc., on the inductors' self-capacitance and calculation accuracy, have all been considered. The calculated equivalent lumped stray capacitance for a rod inductor with ferrite core is compared to that estimated from measurement. Good agreement between them has been observed.

I. INTRODUCTION

The stray capacitance of an inductor (or choke), widely used for suppressing radio-frequency (RF) noise, plays an important role in affecting the frequency characteristic and performance of the inductor. Therefore, its modeling is essential for accurate inductor equivalent circuit modeling and very useful for characterizing the inductor. It helps identify the key factors that affect the value of the lumped stray capacitance of the inductor and improve inductor design.

The bulk rod inductor used for noise suppression typically consists of a *single-layer* winding which is made of a round copper wire wound on a *slug-type ferrite core*. The parasitic capacitance between the winding turns appears in shunt with the inductor and results in the occurrence of resonance at some frequency [1]. Above this self-resonant frequency, the impedance of the inductor becomes predominantly capacitive.

Massarini and Kazimierczuk [2] derived expressions for calculating the self-capacitance of single-layer and multiple-layer inductors with and without a conductive core, including an analytical equation for calculating the capacitance between two *adjacent air-core* turns. Their equations ignore small variations in turn-to-turn capacitance caused by the existence of nearby turns; that is, the turn-to-turn capacitance calculated by these equations is independent of the relative position of turns in the coil. Coils with dielectric cores were also not considered. Because of the difficulty in accurately estimating the actual paths of electric field lines and the surface area, the analytical expressions of the capacitance given in [2] might underestimate the self-capacitance by 10% to 40%.

At RF, the direct measurement of the stray capacitance of an inductor is difficult. In [3], a technique was developed for estimating the shunt self-capacitance of a ferrite-core inductor and its other equivalent circuit parameters.

In this paper, a study on the stray capacitance modeling of a single-layer slug-type inductor with a ferrite core has been conducted by using the finite element method (FEM) and a lumped node-to-node capacitance network method. The lumped stray capacitance calculated by the proposed method is compared with that estimated by the measurement method given in [3]. The correlation between them is very good.

*This work was done while the authors were with the Body & Electrical Systems, ITT Automotive, Inc. (now Valeo Inc.), Dayton, OH.

II. INDUCTOR SELF-CAPACITANCE MODELING

An inductor can be modeled by an equivalent circuit at RF as shown in Figure 1, where R_L, L_L and C_S are, respectively, the equivalent resistance, inductance and lumped capacitance of the inductor [1]. R_L is mainly caused by winding and core losses, and C_S represents the distributed turn-to-turn parasitic capacitance effects of the winding. In Figure1, the effects of the ground on the inductor's stray capacitance are ignored. As a result, this model is appropriate only for the cases where there are no grounded conductors nearby, or the coil-to-ground stray capacitance is negligible. Otherwise, a π circuit model for the stray capacitance (see Section II (C)) has to be used. At higher frequencies, some other models might have to be used, such as the transmission line model, for predicting high-frequency behavior of inductors with multiple resonant modes [4].

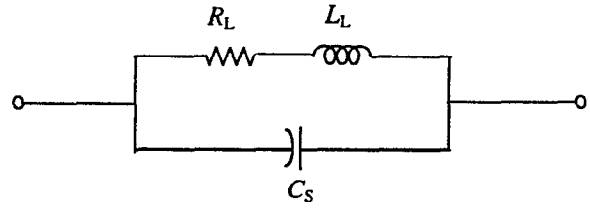

Figure 1. The equivalent circuit model of an inductor.

The stray capacitance of a coil consists of coil turn-to-turn capacitance, turn-to-ground capacitance between coil turns and ground conductors, and turn-to-core capacitance between coil turns and core if the core material is conductive.

In the following, the methods for calculating the turn-to-turn and turn-to-ground capacitance, modeling the distributed stray capacitance and obtaining the equivalent lumped stray capacitance of the inductor are described in details.

A. Calculation of Stray Capacitance of the Inductor by FEM

The turn-to-turn and turn-to-ground capacitances of a single-layer ferrite-core rod inductor are calculated by a 2D electrostatic axisymmetric finite element model. In the 2D axisymmetric model, a helical coil is modeled by a number of coaxial planar loops as shown in Figure 2. The number of the loops is equal to the number of turns and the distance between the centers of two loops is equal to the pitch of the coil. The left edge of the problem outer region, which

passes through the axis of the inductor, is treated as an axisymmetric boundary. The other three edges of the outer region are assigned as balloon-type open boundaries which simulate the infinite large boundaries where either the potential or charge equals zero. Other interfaces between objects are treated as natural boundaries. Triangular cells are used to mesh the whole problem region.

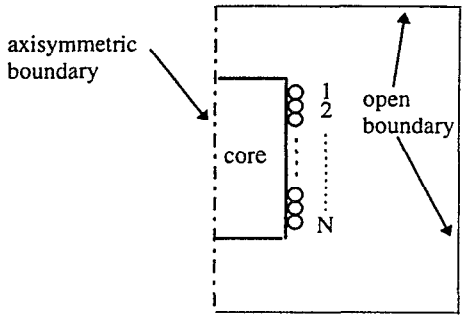

Figure 2. The 2D axisymmetric finite element model of an N-turn inductor.

Maxwell 2D and 3D field simulators are FEM packages from Ansoft Corporation [5], [6]. In *Maxwell* electrostatic simulators which are used as the solvers here, the capacitance between a conductor and other conductive structures or conductors is calculated by: (1)applying one volt to the conductor and zero volts to the other conductive structures; (2)calculating the scalar electric potential ϕ by using the FEM; (3)computing the electric field strength and the electric flux density from ϕ; and (4)obtaining the capacitance values by computing the energy stored in the field.

B. Distributed Stray Capacitance Modeling

The distributed capacitance of an inductor is modeled by a network of lumped node-to-node capacitance elements as given in Figure , where each node represents a turn.

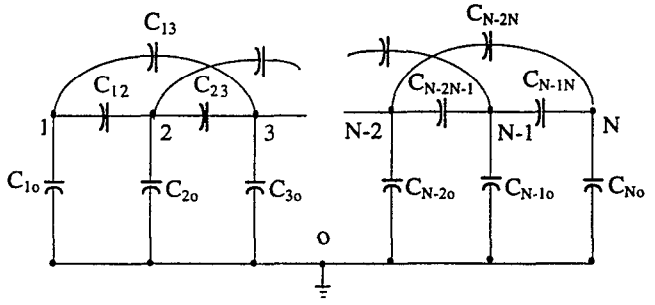

Figure 3. The node-to-node lumped capacitance network.

In Figure , the symbol C_{ij} represents the capacitance between the turns i and j, and C_{io} gives the total capacitance of the turn i to ground. The relationship among the node voltages, node currents and node-to-node capacitance can be represented by an $N \times N$ admittance matrix (see Eq. 1), where the turn-to-core capacitance and the capacitance between the coil and other conductors are ignored. In (1), I_i, V_j and Y_{ij} are current, voltage and admittance, respectively, where $i, j = 1 \ldots N$. Eq. 1 gives a general expression about the capacitive couplings among conductors. In practice, for the turn k, only its coupling with the turn $k-2$, $k-1$, $k+1$ and $k+2$ need to be taken into account and others can be ignored. In other words, in the admittance matrix, $Y_{k,j}=0$ where $j \neq k$, $k-2$, $k-1$, $k+1$and $k+2$. If other nearby conductors including the core exist, more nodes need to be added to the network shown in Figure .

$$\begin{bmatrix} I_1 \\ I_2 \\ \vdots \\ \vdots \\ I_N \end{bmatrix} = \begin{bmatrix} Y_{11} & Y_{12} & \cdots & \cdots & Y_{1N} \\ Y_{21} & Y_{22} & \cdots & \cdots & Y_{2N} \\ \vdots & \vdots & \cdots & \cdots & \vdots \\ \vdots & \vdots & \cdots & \cdots & \vdots \\ Y_{N1} & Y_{N2} & \cdots & \cdots & Y_{NN} \end{bmatrix} \begin{bmatrix} V_1 \\ V_2 \\ \vdots \\ \vdots \\ V_N \end{bmatrix}. \quad (1)$$

For a coil turn, the existence of nearby conductors or coil turns will affect its charge distribution. Therefore, the assumption $C_{i,i+k}=C_{i+j,i+j+k}$ is not always valid. If the inductor and its surrounding objects are symmetric about the inductor center plane which is perpendicular to the inductor center axis, the calculations for the turn-to-turn capacitance can be reduced half.

Inductors used in EMI noise filtering circuit generally have small number of turns. The calculation of the turn-to-turn capacitance by a 2D electrostatic axisymmetric FEM is very fast. For an inductor with 11 turns, the real computation time for the above admittance matrix is about 30 seconds and the CPU time is about 10 seconds with a HP Apollo series 700 workstation.

C. Calculation of Lumped Equivalent Stray Capacitance

The equivalent stray capacitance of an inductor between its two terminals can be obtained by eliminating all intermediate nodes. Here, the reduction of the nodes is done by the appropriate matrix operation. It can also be done by Δ/Y transformation which eliminates one internal node at a time.

Eq. (1) is rearranged as following:

$$\begin{bmatrix} I_1 \\ I_N \\ \hline I_2 \\ \vdots \\ I_{N-1} \end{bmatrix} = \left[\begin{array}{cc|ccc} Y_{11} & Y_{1N} & Y_{12} & \cdots & Y_{1,N-1} \\ Y_{N1} & Y_{NN} & Y_{N2} & \cdots & Y_{N,N-1} \\ \hline Y_{21} & Y_{2N} & Y_{22} & \cdots & Y_{2,N-1} \\ \vdots & \vdots & \vdots & \vdots & \vdots \\ Y_{N-1,1} & Y_{N-1,N} & Y_{N-1,2} & \cdots & Y_{N-1,N-1} \end{array}\right] \begin{bmatrix} V_1 \\ V_N \\ \hline V_2 \\ \vdots \\ V_{N-1} \end{bmatrix}. \quad (2)$$

Then (2) becomes,

$$\begin{bmatrix} I_x \\ I_y \end{bmatrix} = \begin{bmatrix} Y_{xx} & Y_{xy} \\ Y_{yx} & Y_{yy} \end{bmatrix} \begin{bmatrix} V_x \\ V_y \end{bmatrix}, \quad (3)$$

where the corresponding vector and matrix partitions can be readily identified,

$$[I_x] = \begin{bmatrix} I_1 \\ I_N \end{bmatrix}, \qquad [V_x] = \begin{bmatrix} V_1 \\ V_N \end{bmatrix},$$

$$[I_y] = \begin{bmatrix} I_2 \\ \vdots \\ I_{N-1} \end{bmatrix}, \qquad [V_y] = \begin{bmatrix} V_2 \\ \vdots \\ V_{N-1} \end{bmatrix},$$

$$[Y_{xx}]=\begin{bmatrix} Y_{11} & Y_{1N} \\ Y_{N1} & Y_{NN} \end{bmatrix},\quad [Y_{xy}]=\begin{bmatrix} Y_{12} & \cdots & Y_{1N-1} \\ Y_{N2} & \cdots & Y_{NN-1} \end{bmatrix},$$

$$[Y_{yx}]=\begin{bmatrix} Y_{21} & Y_{2N} \\ \vdots & \vdots \\ Y_{N-11} & Y_{N-1N} \end{bmatrix} \text{ and } [Y_{yy}]=\begin{bmatrix} Y_{22} & \cdots & Y_{2N-1} \\ \vdots & \vdots & \vdots \\ Y_{N-12} & \cdots & Y_{N-1N-1} \end{bmatrix}.$$

When $I_y = 0$, it can be derived from (3) that

$$V_y = -Y_{yy}^{-1}Y_{yx}V_x. \tag{4}$$

Substituting (4) into (3) yields that

$$I_x = (Y_{xx} - Y_{xy}Y_{yy}^{-1}Y_{yx})V_x = Y_xV_x, \tag{5}$$

where Y_x is a $2x2$ matrix and has the form

$$Y_x = Y_{xx} - Y_{xy}Y_{yy}^{-1}Y_{yx}.$$

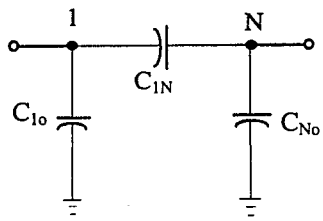

Figure 4. The equivalent circuit of the inductor between two terminals.

Then, after eliminating all intermediate nodes, the equivalent circuit of the inductor between its two terminals is given in Figure 4. The non-diagonal admittance in Y_x matrix is equal to $-j\omega C_{1N}$. Hence, the equivalent stray capacitance between the two terminals of the inductor can be obtained easily.

III. CALCULATION RESULTS

The accuracy of calculating the turn-to-turn capacitance by the electrostatic 2D axisymmetric FEM has been evaluated by comparing the calculation results with those of an electrostatic 3D model. The effects of conductor insulation layer, ferrite core, modeling methods, number of segments for modeling the circumference of a circular wire cross section, types of open boundary condition used, presence of nearby conductors, and capacitance between non-adjacent turns, on the stray capacitance and calculation accuracy have also been studied.

A. *Sample Inductors*

Four single-layer rod sample inductors were used in this study. The windings of all sample inductors are made of round copper wires with a diameter of 1.59 mm and have the same mean radius of the conductor loop which is 3.4 mm and the same pitch distance, i.e., the distance between the centers of two adjacent turns, which is equal to 1.73 mm. The sample inductors used include

- COIL1: an *air-core* coil which consists of two coaxial toroidal loops made of bare wires.
- COIL2: a two-turn *air-core* helical coil made of bare conductors.
- COIL3: an 11-turn *air-core* helical inductor. The dielectric constant of the conductor insulation is 4. The thickness of the conductor insulation is 0.07 mm.
- COIL4: an 11-turn *ferrite-core* helical inductor. Its core is made of Fair-Rite #43 soft ferrite material with an RF dielectric constant 14 and conductivity about 10^{-3} $(\Omega\cdot m)^{-1}$. The length of the core is 21.44 mm and the radius of the core is 2.54 mm. Its winding has the same properties and geometry as that of the COIL3.

A 70 mm × 100 mm outer boundary (see Figure 2) was applied to all following 2D model studies.

B. *Parametric Analysis*

Appropriate Number of Segments for Modeling a Round Wire

As mentioned before, *Maxwell* 2D electrostatic field solver was used to calculate the inductor stray capacitance, such as the turn-to-turn and turn-to-ground capacitance. In the *Maxwell* 2D field simulator, a circle is modeled by a polygon. The number of sides of the polygon affects the size of the wire meshes. Therefore, the number of segments per circumference of the conductor cross section is important for obtaining accurate turn-to-turn capacitance. It is obvious that *the overall distance between turns decreases as the number of sides of the polygon increases*. The stray capacitance thus increases with the increase in number of segments used.

For example, for COIL3, the capacitance between the turn 1 and turn 2 C_{12} increases 60% when the number of segments per conductor circumference is increased from 8 to 32.

Table 1. Turn-to-turn Capacitance of Coil1 vs. the Various Number of Segments per Conductor Circumference by Using 2D Axisymmetric Finite Element Model.

Number of Segments per Conductor Circumference	Turn-to-turn Capacitance (pF)
8	1.14
16	1.32
32	1.39
64	1.41
128	1.42

In order to identify the appropriate number of segments for modeling a round conductor in terms of capacitance calculation, a test case was run for COIL1 with various number of segments, where the charge-type balloon open boundary condition was used. The results are tabulated in Table 1. The geometry of COIL1 is rotationally symmetric about its center axis. The 2D axisymmetric FEM thus should be able to deliver accurate results if the mesh size is segment appropriate. From Table 1, it can be seen that when the number is changed from 16 to 32, the turn-to-turn capacitance increases 5.3%. However, when the number of segments is further increased from 32 to 64, the turn-to-turn capacitance increases only 1.44%. There is always a trade-off between the number of segments per wire circumference used and the computation time. Therefore, *the appropriate number of segments per circumference of a round wire is around 32.*

2D Modeling vs. 3D Modeling

Theoretically speaking, the 3D modeling for a device is more accurate than its 2D modeling. The geometry of a device can be modeled more accurately in its 3D modeling. However, the accuracy of 3D modeling is limited by available computer resources and numerical techniques.

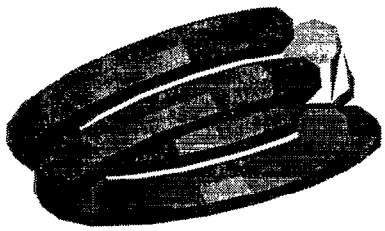

Figure 5. The 3D finite element model of COIL2.

For the purpose of comparing the computation accuracy, the turn-to-turn capacitance of COIL2 was calculated by a 3D FEM with *Maxwell* 3D electrostatic field solver. In the 3D finite element model, a helical coil is *artificially* broken into a number of helical turns as shown in Figure 5. This can be done by artificially reducing the length of one turn or the length of both turns slightly, e.g., 1.0% for one turn or 0.5% for both turns. The shortening of the coil turns will give a gap of about 3.6 degree between two adjacent turns. The cross section of the wire is modeled by a polygon, like in 2D model. A cylinder which surrounds the object was created and used as the problem boundary. The surfaces of the problem outer region are treated as Neumann boundaries, that is, the electric field is tangential to those surfaces and the charge on those surfaces is zero (the open boundary options are not available in *Maxwell* 3D solver). The results are given in Table 2, where the height and radius of the background cylinder that forms the boundary are 24 mm and 13 mm, respectively.

Table 2. Turn-to-turn Capacitance of Coil2 vs. the Various Number of Segments Per Wire Circumference and Segments Per Turn, Respectively, by Using 3D Finite Element Model.

Number of Segments per Conductor Circumference	Turn-to-turn Capacitance (pF)	
	Number of Segments per Turn =16	Number of Segments per Turn = 32
8	1.11	1.17
16	1.29	1.35

For COIL2, its 2D axisymmetric finite element model is same as that of COIL1. Its turn-to-turn capacitance is given in Table 2.

There is a difference in the mean circumference of a planar ring conductor and a helical conductor. However, for a tightly wound coil, such difference is small, and can be neglected.

By comparing the results given in Table 1 and Table 2, it can be seen that the error between the results of the 2D and 3D modeling methods is 2.3% with 16 segments per wire circumference. Therefore, it can be concluded that the 2D axisymmetric model is reasonably accurate for calculating the turn-to-turn capacitance of a helical coil.

Effects of Conductor Insulation Layer

Including the wire insulation layer into the model is crucial for obtaining accurate capacitance, especially for tightly wound coils. For a tightly wound winding, the only space between two adjacent conductors is their insulation layer. Therefore, the insulation layer is the major medium for forming the turn-to-turn stray capacitance between the two adjacent turns.

For example, for COIL3, if its conductor insulation layer is not considered in its 2D axisymmetric model, its turn-to-turn stray capacitance C_{12} is 38% lower than that if the insulation layer is taken into consideration. In both cases, 8 segments were used for modeling the conductor circumference.

Effects of Core Materials

For an inductor with a core whose relative permittivity is not one, the dielectric core should be included in the model. The existence of the dielectric core will increase the coupling between turns. Hence, the stray capacitance between turns, especially for non-adjacent turns, will increase.

The only difference between COIL3 and COIL4 is that COIL4 has a dielectric core and COIL3 does not. A capacitance calculation was thus conducted for COIL3 and COIL4, respectively, by using the 2D modeling method. In both cases, 32 segments per wire circumference were used. For COIL3, the calculated turn-to-turn capacitance C_{12} = 2.57 pF and C_{13} = 0.046 pF and the equivalent lumped stray capacitance is 0.439 pF. For COIL4, the calculated turn-to-turn capacitance C_{12} = 2.95 pF and C_{13} = 0.19 pF, and the equivalent lumped stray capacitance of COIL4 is 0.563 pF. Therefore, for inductors with soft ferrite cores, e.g., nickel zinc ferrites whose RF relative permittivity is 14, the core must be simulated in the model. Otherwise, the stray capacitance might be underestimated.

The conductivity of the core material will also affect the coil stray capacitance. Generally, the conductivity of nickel zinc soft ferrites is very low, around 10^{-7} to 10^{-3} $(\Omega\cdot m)^{-1}$. For a manganese zinc or manganese soft ferrite, its conductivity usually is in the range of 0.5 to 2 $(\Omega\cdot m)^{-1}$ [7]. For other types of core materials, the conductivity of the core might be higher. Just for verification purpose, let the conductivity of COIL4 be changed from 10^{-3} $(\Omega\cdot m)^{-1}$ to 10^{4} $(\Omega\cdot m)^{-1}$. Then, the turn-to-turn capacitance C_{12} is changed from 2.95 pF to 2.49 pF, and C_{13} is changed from 0.19 pF to 3.44×10^{-2} pF, with 32 segments per conductor circumference used. It is obvious that with the increase in conductivity of the core material, the turn-to-turn capacitance will be reduced slightly. In addition, the turn-to-core capacitance will increase significantly [2].

Effects of the Capacitance between Non-adjacent Turns

The non-adjacent turn-to-turn capacitance and turn-to-ground capacitance should be considered in the calculation of the total lumped capacitance, if their values are comparable with their adjacent turn-to-turn capacitance values. In the literature related to the coil self-capacitance calculations, many authors assume that the stray capacitance between non-adjacent turns can be ignored in the total equivalent capacitance calculation [2]. This might be true only for a loosely wound air-core coil. Otherwise, the equivalent lumped stray capacitance will be underestimated.

A test was run for calculating the equivalent lumped stray capacitance of both COIL3 and COIL4, with and without the non-adjacent capacitance taken into account. In the turn-to-turn stray

capacitance calculation, 2D axisymmetric modeling method was used with 32 segments per conductor circumference. For COIL3, whose maximum capacitance between non-adjacent turns is two orders lower than that between adjacent turns, the calculated equivalent stray capacitance is 0.439 pF when the non-adjacent turn-to-turn capacitance is included in the node-to-node lumped capacitance network model of the coil. However, if all non-adjacent turn-to-turn capacitance is ignored, the calculated equivalent capacitance becomes 0.253 pF. Therefore, ignoring the non-adjacent turn-to-turn capacitance for COIL3 gives a calculation error of 42.4%. For COIL4, its non-adjacent turn-to-turn capacitance is higher than that of COIL3 due to the existence of the ferrite core and the maximum value is one order lower than the adjacent turn capacitance. If only considering adjacent turn-to-turn capacitance in the model, the calculated equivalent stray capacitance is 0.286 pF, which is much lower than the total lumped capacitance of 0.563 pF with non-adjacent turn-to-turn capacitance included in the model. For COIL4, this gives a calculation error of 49.2%.

Effects of Nearby Conductors

Due to proximity effects, the existence of nearby conductors affects the distributed stray capacitance. This reduces the lumped series stray capacitance of the inductor, but increases the coil-to-ground capacitance. Therefore, they must be included in the model.

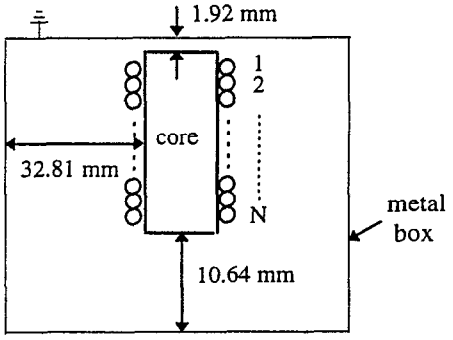

Figure 6. The geometry of COIL4 surrounded by a grounded metal box.

Giving an example, if COIL4 is surrounded by a grounded cylindrical metal box as shown in Figure 6, it can be seen from the calculation that the stray capacitance of COIL4 will be changed, as expected. The turn-to-turn capacitance changes slightly, but the turn-to-ground capacitance increases significantly, where in the calculation the number of segments per wire circumference equals 32. Referred to Figure 4, the equivalent series stray capacitance $C_{1,11}$ reduces from 0.563 pF to 0.314 pF and the equivalent C_{1o} and $C_{11,o}$ increase to 0.679 pF and 0.502 pF, respectively.

Effects of Pitch and Coil-to-Core Distance

Both the pitch distance and the distance between core and coil affect the stray capacitance significantly, especially the former. The stray capacitance increases with the decrease of those distances.

A test case was run for COIL4 with various pitch distances by using the 2D modeling method. The turn-to-turn capacitance C_{12} for different coil pitch distances is shown in Table 3, where 32 segments per wire were used in the calculation. It can be seen that when the coil pitch distance is increased, the space between turns is increased and thus the stray capacitance is reduced accordingly.

Table 3. The Calculated Turn-to-turn Stray Capacitance C_{12} of Coil3 vs. the Pitch Distance of the Coil.

Pitch (mm)	Turn-to-turn space (mm)	C_{12} (pF)
1.73	0	2.57
1.80	0.07	1.50
1.87	0.14	1.14

For COIL4, if the diameter of the core is reduced slightly, e.g., 0.005 mm, then a very small air gap is inserted between the core and the winding. Then the turn-to-turn capacitance C_{12} is changed from 2.98 pF to 2.95 pF and C_{13} is changed from 0.196 pF to 0.194 pF, and the total stray capacitance is reduced slightly to 0.560 pF from 0.563 pF, where the number of segments per conductor circumference equals 32. This indicates that the self-capacitance can be reduced slightly by increasing "air" space between the coil and core.

Effects of the Type of Open Boundary Condition

There are two different types of open boundary conditions. One is charge-type open boundary condition, where the total charge on the open boundary is zero. The other type is the voltage-type open boundary condition, where the potential on the open boundary is zero. The choice of different types of open boundary conditions in the model will give different turn-to-ground capacitance and slightly different turn-to-turn capacitance. For the charge-type open boundary condition, the turn-to-ground capacitance usually is very small and can be ignored if there are no grounded conductors nearby, that is, in Figure 3, $C_{io} \cong 0$ (i=1, ..., N). For the voltage-type open boundary condition, the turn-to-ground capacitance usually can not be ignored in the node-to-node capacitance network.

Generally, the charge-type open boundary condition is appropriate for most applications and should be used.

C. *Comparison with Measured Results*

As mentioned above, the equivalent lumped series stray capacitance of COIL4 calculated by the 2D modeling method presented in this paper is 0.563 pF, where there are no other grounded conductors nearby.

The equivalent lumped stray capacitance of two sample inductors of COIL4 was also estimated by using the measurement method described in [3].

The stray capacitance of an inductor can be estimated by measuring the resonant frequencies of the inductor circuit with external capacitors in parallel with the inductor, as shown in Figure 7, where C_{ext} is the capacitance of the external capacitor. The lumped stray capacitance can be estimated by the following equation:

$$C_S = C_1 \cdot \frac{\frac{C_2}{C_1} \cdot \left(\frac{f_2}{f_1}\right)^2 - 1}{1 - \left(\frac{f_2}{f_1}\right)^2}, \qquad (6)$$

where C_1 and C_2 are the capacitance of two external capacitors, f_1 is the resonant frequency of the circuit with C_1 in parallel with the inductor and similarly, f_2 is the resonant frequency of the circuit with C_2 in parallel with the inductor.

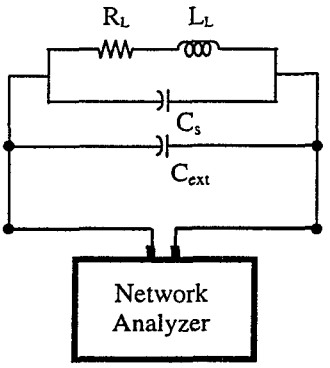

Figure 7. Measurement setup diagram.

Table 4. Comparison Between The Calculated And Estimated Equivalent Lumped Stray Capacitance Of Coil4

Calculated	Estimated from Measurement	
	Sample 1	Sample 2
0.563 pF	0.539 pF	0.573 pF

The two external capacitors used in the measurement are 3.31 pF and 5.53 pF, measured by HP 4276 LCZ meter at 20 kHz. HP 8753B network analyzer was used to measure the resonant frequency of the inductor circuit. The measured and calculated equivalent lumped stray capacitance of COIL4 are tabulated in Table 4. Good agreement between the calculated and measured results has been observed. The discrepancy between them is about 1.7% to 4.5%.

IV. CONCLUSIONS

This paper proposed a method for modeling the self-capacitance of rod inductors. The 2D axisymmetric finite element method was used to calculate the stray capacitance of the inductor, and the lumped node-to-node capacitance network was used to model the distributed capacitance of the inductor. Four samples inductors were used in the studies. The calculation results are compared with the estimated ones from measurement. Good agreement has been observed. In addition, a thorough parametric analysis has been conducted, which includes studying the effects of number of segments for modeling a round conductor, insulation layer, core material, pitch distance, coil-to-core distance, non-adjacent turn-to-turn capacitance, etc., on the stray capacitance and its calculation.

REFERENCES

[1]. Henry W. Ott, *Noise Reduction Techniques in Electronic Systems*, John Wiley & Sons, 2nd Edition, 1988.

[2]. Antonio Massarini and Marian K. Kazimierczuk, "Self-Capacitance of Inductors", *IEEE Trans. On Power Electronics*, Vol. 12, No. 4, pp. 671-676, 1997.

[3]. Qin Yu, Thomas W. Holmes, and Krishna Naishadham, "Radio Frequency Characterization of Ferrite Materials", *IEEE AP-S International Symposium and URSI North American Radio Science Meeting*, 106.03, 1997.

[4]. Randall W. Rhea, "A Multimode High-Frequency Inductor Model", Applied Microwave & Wireless, Vol. 9, No. 6, pp. 70-80, 1997.

[5]. *Maxwell 2D Simulator User's Reference*, Ansoft Corp.,1994.

[6]. Maxwell *3D Simulator User's Reference*, Ansoft Corp.,1993.

[7]. *Fair-Rite Soft Ferrites*, 13th edition, Fair-Rite Products Corp., 1996.